

Chapter 14

Study and Estimation of Static Stiffness of Machine Tool Spindle



Vibish S. Bhardwaj, Ramesh H. Aralaguppi, Ashok N. Badhe, Bhargav and Arun R. Rao

Abstract Spindle stiffness is the ability of spindle to resist deformations under the influence of cutting forces. The magnitude of deflections at the spindle nose, where cutting forces from the tool are transmitted, decides the machining accuracy of the machine tool. In this paper, a method to evaluate the static stiffness of the spindle with a bearing system subjected to cutting force is presented. The static stiffness of the spindle is calculated analytically by evaluating the radial stiffness of the bearings and the deflection at the front end of the spindle. Finite Element Analysis is carried out on the spindle bearing system, and results are compared with analytical results. Further, experiments are carried out to validate the analytical and numerical results.

Keywords Bearing force components · Static stiffness of spindle bearing system · Finite element analysis · Experimental setup

14.1 Introduction

Machine tools are used to produce high precision components in a short time with greater accuracy. The global market demands for very low machining tolerances. The stiffness of the machine tool spindle plays a very important role in achieving higher machining accuracy. Accuracy of machining operations depends on the cutting forces and the deflections caused on the spindle. For a spindle to take both radial and axial forces, it is important to select appropriate bearings and their arrangements. The optimum bearing arrangement contributes to the stability, working accuracy, revolving speed and stiffness of the spindle bearing system. Bearing arrangement of the spindle system affects the surface profile, quality and dimensional accuracy of the manufactured parts. Static stiffness decides the deflection the spindle undergoes when

V. S. Bhardwaj · Bhargav (✉) · A. R. Rao
Department of Mechanical and Manufacturing Engineering, M. S. Ramaiah University
of Applied Science, Bengaluru, India
e-mail: 93.bhargav@gmail.com

R. H. Aralaguppi · A. N. Badhe
Dr. Abdul Kalam Center for Innovation, Bharat Fritz Werner Ltd., Bengaluru, India

© Springer Nature Singapore Pte Ltd. 2020
M. Vinyas et al. (eds.), *Advances in Structures, Systems and Materials*,
Lecture Notes on Multidisciplinary Industrial Engineering,
https://doi.org/10.1007/978-981-15-3254-2_14

a static force is acting on the spindle nose. When the operating frequency of these high-speed spindles falls under the resonant zone, the amplitude of vibration in the spindle will reduce the stiffness of the spindle bearing system considerably. Hence, stiffness estimation of spindle with the bearing system in the static and dynamic conditions is very important.

Shuzi [1] discussed the significance of the radial stiffness during static stiffness analysis of a spindle bearing system. Influences of various spindle parameters like bearing span length, overhang and bearing stiffness are studied. The bearing reaction forces are derived from direct and indirect influence methods, and relations for spindle stiffness with two and more bearing supports are arrived. To enhance the static stiffness of the spindle, the stiffness of the front bearing, area moment inertia of the spindle and reduction in the spindle overhang length are important. However, there are no experimental validations made for the suggested methods. Sarenac [2] studied the methods of creating a rigid spindle by optimizing the spindle parameters. Paper suggests the ratio of bearing span length to the spindle overhang which can help to decide the spindle stiffness. It also suggests that the higher spindle stiffness can be achieved by improving the stiffness of the bearing and spindle cross section. Kutlu [3] worked on the performance requirements of a machine tool spindle by considering high loads concentrated on the spindle nose and analyzing the static and dynamic stiffness of the spindle. The static stiffness is arrived by the superposition method for the spindle bearing system, and the analytical values are verified with FEA results. Soos [4] estimated the deflection on the spindle nose by considering the spindle bearing system divided into nodes and solving analytically as the static parameters. The bending moments on the overhang and the deflection due to bearing compliances are used to estimate the deflections at the spindle nose. Prakosa and Wibowo [5] built a mathematical model of the spindle bearing system and studied the stiffness results by changing the bearing preload, span length, number of bearing and spindle length. Later, they optimized these parameters to improve the stiffness. Using Dunkley's method, the resonating frequencies are obtained and compared with experimental results.

In this paper, a methodology to estimate the static stiffness of the machine tool spindle is developed. Radial deflection of the spindle is determined by considering the bearing compliance when it is subjected to cutting forces analytically. The correctness of the analytical deflections is verified numerically by using FEA software. Finally, the deflection results obtained are validated with experimental results.

14.2 Static Stiffness Analysis Using Analytical Approach

In the spindle bearing system, shown in Fig. 14.1, a hollow spindle is supported by angular contact ball bearings which take both axial and radial forces at high speeds. Bearings are arranged in a quad back-to-back arrangement to accommodate axial forces in both directions. The static stiffness of the spindle bearing system under the

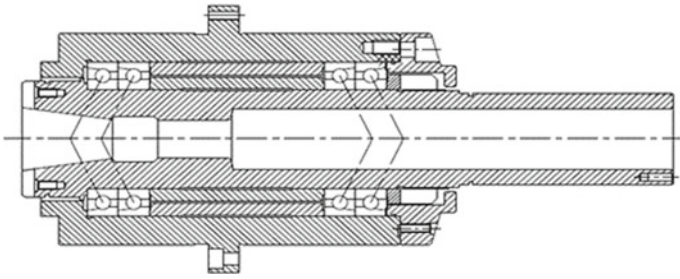


Fig. 14.1 Schematic of spindle bearing system

influence of cutting forces transmitted to the spindle nose during milling operations is evaluated.

14.2.1 An Evaluation of Axial and Radial Forces on Bearing Compliance

The axial force is acting parallel to the spindle axis due to the preload applied on the bearings using a locknut. Tightening torque is applied on the locknut to provide necessary preload on the bearings. The axial force is derived from the tangential force generated by the locknut [6]. The relation between the axial force and the tightening torque is shown in Eq. (14.1).

$$F_A = \frac{T}{(0.16662d)} \quad (14.1)$$

where T is the tightening torque, d is the effective diameter of the locknut, 0.16662 is the locknut pitch angle factor, and F_A is the axial force acting on the bearing. Radial forces are acting perpendicular to the axis of the shaft. When the cutting forces are transmitted to the spindle nose during milling operation, it creates reaction force at the bearings as shown in Fig. 14.2. Reaction forces acting in the radial direction are arrived using moment and equilibrium equations. Reaction forces at the front bearing FR1 and the rear bearing FR2 are evaluated. From Fig. 14.2, it can be observed that due to the cutting forces acting on the spindle nose, a reaction force FR1 acts in the upward direction on the front bearing and reaction force FR2 acts in the downward direction on the rear bearing.

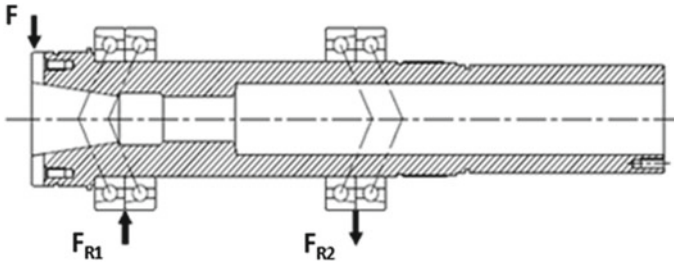


Fig. 14.2 Bearing reaction forces

14.2.2 Bearing Radial Stiffness

Bearing arrangement and the contact angle of the bearing play a major role in deciding its radial stiffness. The radial stiffness of the bearings is evaluated by multiplying the contact angle factor and axial stiffness of the bearing. The axial stiffness value (K_A) and the contact angle (θ_{Factor}) of the bearing are selected from the bearing catalog [7]. The front and rear bearings are of the same dimensions. The relation for the radial stiffness of the bearing is given in Eq. (14.2). Using this equation, the radial stiffness of the bearing is calculated.

$$K_R = K_A * \theta_{\text{Factor}} \quad (14.2)$$

14.2.3 Static Stiffness of Spindle Bearing System

Various methodologies for evaluating deflections at spindle nose when subjected to cutting forces are discussed [3]. Deflections are evaluated using the superposition technique. In the first case, the spindle bearing system is considered to have a rigid shaft with elastic bearings, and in the second case, the system has an elastic shaft with rigid bearings. Both the cases are combined to obtain deflection at spindle nose where the shafts and bearings deform elastically. In another technique [4], the bending moments acting on the spindle bearing system are combined with the deflections caused by the bearing arrangements to evaluate the deflection at the spindle nose.

The spindle system shown in Fig. 14.3 is supported by front and rear bearings, and cutting force P is acting on the spindle overhang section. Deflection at the spindle nose is evaluated using Eq. (14.3) by considering the spindle and its support as elastic bodies to arrive at the real-time deflections [1].

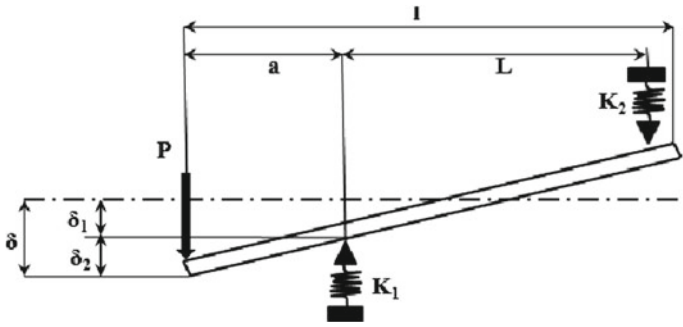


Fig. 14.3 Nature of deflection at the spindle nose

$$\delta = P \left[\frac{a^3}{3EJ_a} + \frac{La^2}{3EJ_L} + \frac{1}{K_1} \left(1 + \frac{a}{L} \right)^2 + \frac{1}{K_2} \left(\frac{a}{L} \right)^2 \right] \tag{14.3}$$

where

- A Spindle overhang
- E Modulus of elasticity
- δ Deflection at spindle nose
- J_a and J_L Area moment of inertia at overhang and bearing span
- L Bearing span length
- P Cutting force
- K_1 and K_2 = Front and rear bearing stiffness.

Assumptions made to evaluate the deflection at the spindle nose are as follows:

- (a) The spindle is a flexible overhang beam body
- (b) The beam is simply supported
- (c) Flexible supports with stiffness values and
- (d) Point load acting at the end of the overhang section.

In Eq. (14.3), the first term signifies the deflections at the overhang section, the second term signifies the deflection at the span length where the spindle acts as a simply support beam, and the remaining terms signify the deflection at the spindle nose due to the deflection of the front and rear bearings. All these deflections act in the radial direction. The sum of these deflections results in the static deflection at the spindle nose as shown in Eq. (14.3). The static stiffness of the spindle bearing system is arrived by using Eq. (14.4).

$$K = P/\delta \tag{14.4}$$

14.3 Finite Element Analysis

A hollow spindle model is developed, and angular contact ball bearings are mounted in a quad back-to-back arrangement with respect to the schematic of the spindle bearing system. COMBIN 14 element type is used to provide radial stiffness to the bearing. Convergence study for results up to 0.1% difference in results is carried out, and discretization of 5 mm based on convergence study is performed. The material properties of steel are specified. Appropriate boundary conditions where the bearings are constrained in all degrees of freedom with respect to the spindle housing are specified, and load is applied in X-axis at the spindle nose as cutting forces. Static structural analysis is carried out using ANSYS Workbench.

14.4 Experimental Setup

Machine tool spindle of a vertical machining center is considered. An experimental setup is made to measure the deflection on the spindle nose due to static load. Static load is applied on the tool holder using a beam load cell as shown in Fig. 14.4 to create a cutting force on the spindle nose. The maximum cutting forces experienced on the machine tool spindle during machining operations is 2000 N. The load cell used here has a capacity of load from 0 to 1000 kg.

A Linear Variable Displacement Transducer (LVDT) with up to 0.1 μ resolution having a magnetic base is used to measure the deflections at the spindle nose and the tool holder. The magnetic base is placed on the stationary part of the spindle unit close to the bearing housing. A gradual incremental load is applied, and the corresponding deflections are measured. One of the LVDT styluses is placed on the spindle nose and the other on the tool holder as shown in Fig. 14.4; the respective deflections are identified. Experimental study is carried out to evaluate the spindle bearing stiffness which is discussed in the next section.

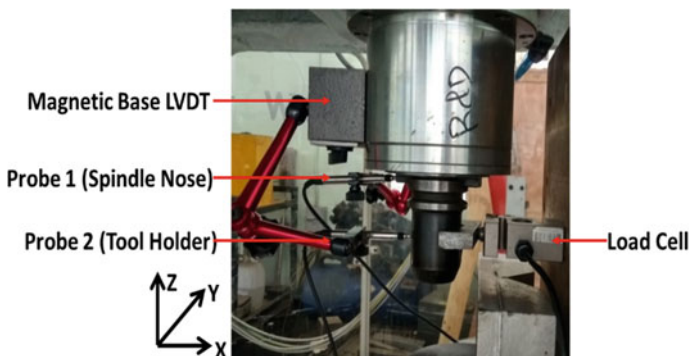


Fig. 14.4 Experimental setup for spindle deflection test

14.5 Results and Discussion

14.5.1 Deflection Result

The deflections on the spindle nose for various external force values applied using a load cell are evaluated analytically using Eq. (14.3). These results are compared with experimental results and FEA results, and differences in terms of percentage are tabulated in Table 14.1.

Table 14.1 shows the percentage difference between the deflections at the spindle nose arrived from analytical and experimental approach. It can be observed that the difference tends to reduce as the externally applied force increases. This is due to the stiffness of the spindle bearing system which resists deflecting the spindle nose more at lesser applied force. The spindle behavior is similar to that of its operating conditions, when it performs machining operations along a particular axis. It can be observed from Sl. No. 5 and onwards in Table 14.1, where the differences are below 10%. The spindle nose deflections are more realistic after this point. A plot of external force versus displacement is plotted as shown in Fig. 14.5a, representing the comparison of displacement values between the analytical and experimental results.

FEA results of the spindle bearing system are used for total deformations. Table 14.1 shows the results for deflection at the spindle nose using a numerical approach. These results are compared with experimental values which are tabulated in Table 14.1. A plot of external force versus displacement is plotted as shown in Fig. 14.5b, representing the comparison of displacement values between FEA and experimental results. Study is performed to estimate the deflection of the spindle

Table 14.1 Comparison between analytical, experimental and FEA results

Sl. No	External force F (N)	Deflection, δ , at spindle nose (μm)			Percentage difference	
		Analytical result	Experimental result	FEA result	Analytical and experiment	FEA and experiment
1	200	1.23	0.50	1.24	59.34	59.82
2	392	2.42	1.20	2.43	50.41	50.80
3	595	3.68	2.37	3.70	35.59	35.96
4	788	4.87	3.87	4.90	20.53	21.08
5	984	6.08	5.47	6.10	10.03	10.33
6	1194	7.38	7.03	7.41	4.74	5.14
7	1386	8.57	8.63	8.62	0.70	0.05
8	1543	9.54	10.17	9.60	6.60	5.91
9	1778	11.0	11.67	11.06	6.09	5.46
10	1968	12.2	13.37	12.24	9.59	9.16

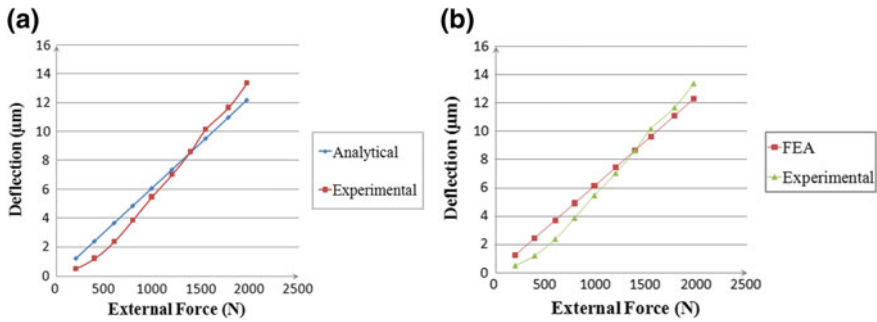


Fig. 14.5 **a** Comparison of analytical versus experimental results. **b** Comparison of FEA versus experimental results

Table 14.2 Deflection results for spindle nose and tool holder

Sl. No.	External force F (N)	Deflection δ (μm)	
		At spindle nose	At tool holder
1	200	0.50	2.03
2	392	1.20	4.63
3	595	2.37	7.87
4	788	3.87	11.07
5	984	5.47	14.40
6	1194	7.03	17.80
7	1386	8.63	21.13
8	1543	10.17	24.23
9	1778	11.67	27.50
10	1968	13.37	30.77

bearing system when a tool holder is attached to the system. Comparisons between experimental deflection at spindle nose and tool holder are tabulated in Table 14.2.

It is noticed that there is a considerable difference in deflection results between both the conditions. Hence, it is also important to evaluate the stiffness of the spindle bearing system with an attached tool holder.

14.5.2 Stiffness Results

The real-time deflections are considered from the point where the difference in results is within 10% (Sl. No. 5 in Table 14.1), and the mean static stiffness of the spindle bearing system for the set of force and deflection values is evaluated using the relation in Eq. (14.4) and tabulated in Table 14.3. Since the current work concentrates on the deflections in the spindle nose, the deflection at tool holder is not considered for

Table 14.3 Static stiffness of spindle bearing system

Methodology	Static stiffness of spindle bearing system (N/ μm)
Analytical	162.92
Finite Element Analysis	160.80
Experimental (At spindle nose)	166.53

further calculations. The experimental static stiffness of the spindle bearing system considering attached tool holder is compared with the static stiffness of the spindle bearing system without tool holder.

From Table 14.3, it is observed that the difference between the static stiffness results at the spindle nose is 2.83% between analytical and experimental results and 3.44% between FEA and experimental results. This indicates that various approaches used, as shown in Table 14.3, for the stiffness analysis yield similar results. Thus, the analytical and FEA results are validated with the experimental values. The static stiffness of the spindle nose reduces due to joint stiffness between the spindle nose and the tool holder when it is attached with tool holder.

14.6 Conclusions

The machining accuracy and working performance of a machine tool directly depend upon tool deformation under operating condition. This deformation depends upon the stiffness of the spindle, and the evaluation of this stiffness is very important. In this paper, a methodology to arrive at the spindle bearing stiffness by identifying the force components acting on the system is proposed. The deflection of the spindle nose is evaluated analytically, numerically and validated with experimental data. The differences in total deformations between the three methods are within 10%. The stiffness of the spindle bearing system is evaluated using the three approaches. The difference in results between analytical and experimental approaches is 2.83% and between numerical and experimental results is 3.44%. Deflections from the tool holder are also measured experimentally. The stiffness of the spindle unit at tool holder point reduces to 72 N/ μm due to joint stiffness between the tool holder and spindle. Future studies to identify the joint stiffness between the spindle nose and the tool holder need to be carried out.

Acknowledgements Authors are thankful to the member organization (Dr. Abdul Kalam Center for Innovation, Bharat Fritz Werner Ltd., Bengaluru, and M. S. Ramaiah University of Applied Sciences, Bengaluru) for supporting this work and Advanced Machine Tool Testing Facility (AMTTF) for supporting with the experimental setup and measurements.

References

1. Shuzi, Y.: A study of static stiffness of machine tool spindles. *Int. J. Mach. Tool Des.* **21**(1), 23–40 (1980)
2. Sarenac, M.: Stiffness of machine tool spindle as a main factor for treatment accuracy. *Sci. J. Facta Univ.* **1**(6), 665–674 (1999)
3. Asimkutlu.: Design and development of a lathe spindle. Master of science thesis, Stockholm (2016)
4. Lubomír, S.: Radial ball bearings with angular contact in machine tools. IntechOpen Ltd., London (2012)
5. Prakosa, T., Wibowo, A., Llhamsyah, R.: Optimizing static and dynamic stiffness of machine tools spindle shaft for improving machining product quality. *J. Kones Powertrain Transp.* **20**(4), 363–370 (2013)
6. IBC High precision locknuts. <http://www.ibc-waelzlager.com>. Last accessed 24 May 2018
7. NSK.: Machine tool spindle bearing selection and mounting guide, England (2009)